sciendo

Radiolytic synthesis of gold nanoparticles in HEMA-based hydrogels: Potentialities for imaging nanocomposites

Katsiaryna Dziarabina,
Uliana Pinaeva,
Sławomir Kadłubowski [ID],
Piotr Ulański [ID],
Xavier Coqueret [ID]

Abstract. This article reports on the radiolytic synthesis of nanocomposites containing gold nanoparticles (AuNPs) within two types of hydrogels based on 2-hydroxyethyl methacrylate (HEMA): (i) plain networks with various contents in ethylene glycol dimethacrylate (EGDMA), as a cross-linker and (ii) stimuli-responsive (SR) networks prepared from these monomers copolymerized with [2-(methacryloyloxy)ethyl]trimethylammonium chloride (MADQUAT) to confer pH-switchable swelling. Hydrogels were prepared by photopolymerization with well-defined composition and a high degree of monomer conversion using two experimental procedures, as xerogels or in aqueous solution. Besides MADQUAT, acrylic acid (AA) or *N*-isopropylacrylamide have been tested as copolymers, yielding pH- or temperature-sensitive hydrogels, respectively. Isothermal swelling in water was affected by monomer composition. Electron beam (EB) irradiation at doses up to 100 kGy of poly(HEMA) xerogels and water-swollen networks prepared with 0.5 wt% of EGDMA had a moderate impact on swelling characteristics and thermomechanical properties of the plain materials, whereas small amounts of extractables were formed. Poly(HEMA)-based nanocomposites containing AuNPs were successfully obtained by EB irradiation of samples swollen by aqueous solutions of Au(III). The effects of dose and cross-linking density on the formation of AuNPs were monitored by UV-visible spectroscopy. Irradiation at well-defined temperatures of the Au(III)-loaded SR hydrogels induced the formation of nanoparticles with size-dependent features, whereas the efficiency of Au(III) reduction at 10 kGy was not significantly affected by the network structure. EB-induced reduction of Au(III) in poly(HEMA) hydrogels using a lead mask to generate well-defined patterns yielded coloured and long-lasting images in the zones where the nanocomposite was formed.

Keywords: Functional hydrogels • Gold nanoparticles • Nanocomposites • Network properties • Radiation--induced reactions • Stimuli-responsiveness

K. Dziarabina
Université de Reims Champagne-Ardenne
Institut de Chimie Moléculaire de Reims
CNRS UMR 7312, BP 1039, 51687 Reims Cedex 2, France
and Lodz University of Technology
Faculty of Chemistry
Institute of Applied Radiation Chemistry
Wroblewskiego 15 Str., 93-590, Lodz, Poland

U. Pinaeva, X. Coqueret✉
Université de Reims Champagne-Ardenne
Institut de Chimie Moléculaire de Reims
CNRS UMR 7312, BP 1039, 51687 Reims Cedex 2, France
E-mail: xavier.coqueret@univ-reims.fr

S. Kadłubowski, P. Ulański✉
Lodz University of Technology
Faculty of Chemistry
Institute of Applied Radiation Chemistry
Wroblewskiego 15 Str., 93-590, Lodz, Poland
E-mail: piotr.ulanski@p.lodz.pl

Introduction

As a part of a project aiming at patterning nanocomposites in hydrogels by radiation-mediated reduction of Au(III) ions into gold nanoparticles (AuNPs), we are currently investigating the synthesis of well--defined poly(HEMA)-based networks and evaluating the potentialities of radiation treatments for creating well-resolved and stable patterns made of AuNPs embedded in hydrogel matrices.

Since the early reports on the structural features and unique properties of metal nanoparticles (NPs) [1–3], various synthetic methods and experimental conditions have been reported in the literature to generate metal clusters starting from metal salts as precursors. Among them, chemical [4, 5] and photochemical [6] redox reactions have been successfully employed, while other highly efficient treatments based on sonication [7] or radiolytic reduction [8–10] have also been developed as greener alternatives. Compared to conventional chemical synthesis, the radiation-induced technique does not

require the use of any reducing agents. Moreover, by adjusting the dose rate, the radiation-induced method provides fine control over the growing rate of metal cluster, which enables therefore to tailor the properties of the reduced nanoparticles because of specific applications.

The radiolytic synthesis is particularly suitable for the generation of metal NPs in aqueous media via the generation of solvated electrons (e^-_{aq}) and hydrogen atoms ($H^{\bullet}$), which can easily reduce metal ions such as, for instance, Au(III), down to zero-valent state [11]. The presence of polymeric solutes may induce a more complex reduction mechanism involving short- and long-lived polymeric species [12, 13]. Nevertheless, the nanocomposite materials consisting of polymer hydrogel network and metallic NPs provide a synergetic effect to the complex material by reducing the risk of nanoparticle aggregation and at the same time enhancing the mechanical strength of the hydrogels. Furthermore, similarly to colloid solutions, the hydrogels containing metal NPs can play the role of reactors catalyzing chemical reactions taking place in aqueous solutions.

Several approaches in polymer/metal NPs synthesis are distinguished. Metal NPs, often functionalized to ensure good solubility in organic media and prevent aggregation, can be directly added to a monomer blend and further converted into a nanocomposite [14] or physically incorporated within an already prepared polymer matrix ("breathing in") [15]. This method, however, is likely to result in an inhomogeneous distribution of NPs. *In situ* chemical metal salt reduction is intended to overcome this issue. For example, Wang *et al.* [16] synthesized a hydrogel made of poly(*N*-isopropylacrylamide) and co-monomers containing thiol groups that may form complexes with Au(III) ions, permitting therefore the formation of uniformly distributed stable and un-aggregated colloidal AuNPs upon addition of sodium borohydride (reducing agent). Alternatively, the radiolytic *in situ* route allows not only size--controllable and uniform nanoparticle generation due to the formation of reducing species with high reduction potentials but also avoids using any undesired chemicals, making the synthesis easier, cleaner, and more versatile. In this approach, the metal salt is either present in a monomer blend so that the metal ion reduction takes place simultaneously with the polymer matrix formation upon irradiation, or added to the pre-formed polymer matrix and then radiolytically processed. Thus, Marić *et al.* [17] reported a one-step synthesis of poly(ethylene oxide) (PEO)/AuNPs nanocomposite hydrogels by γ-irradiation. Authors demonstrated that upon irradiation at 50 kGy and alkaline pH, the hydrogel nanocomposites were produced by simultaneous cross-linking of PEO chains and reduction of Au(III). In the second case, a prepared polymer matrix is allowed to swell in an aqueous metal salt solution before irradiation.

Among the various metal ions that can be reduced in the form of zero-valent nanoparticles, Ag(I) and Au(III) are of the greatest interest due to their nonlinear optical and catalytic properties [18–20]. Despite many successful studies on the

radiolytic formation of AuNPs in aqueous media with [9, 21] and without [22] stabilizing agents such as, for instance, natural polysaccharide chitosan, there are much fewer reports on radiation-mediated metal nanoparticle formation within a hydrogel matrix available. Zhu *et al.* [23] obtained composite poly(NIPAm) hydrogels containing gold nanoparticles by gamma-irradiation-induced polymerization of NIPAm in the presence of gold precursor. Initiation by gamma rays has also been used by Marić *et al.* [17] who obtained hydrogels containing AuNPs by simultaneous cross-linking of PEO and reduction of Au(III) in an aqueous solution. The authors stressed the influence of pH on the character of the final product, concerning both the size of AuNPs and the character of the polymer matrix (continuous hydrogel vs. suspension). A similar approach has been recently applied for synthesizing AuNP/poly(vinyl alcohol) (PVA) gels [24, 25]. Kumar *et al.* [26] have synthesized PVA-AgNPs hydrogel composites by γ-irradiation. It was demonstrated by viscosity measurements that Ag(I) reduction and PVA cross-linking were not taking place simultaneously upon radiolysis, and a complete metal salt reduction (0.2 mM AgNO₃) was achieved at 3.3 kGy resulting in ~20 nm AgNPs. PVA was found to be a very efficient stabilizer to prevent aggregation of the resulted Ag clusters. Henríquez *et al.* [27] reported on *in situ* AgNPs embedded into photopolymerized hydroxyethyl methacrylate (HEMA)-based hydrogels with biocide properties. Krklješ *et al.* [28, 29] synthesized AgNP-containing hydrogels based on PVA. The composites were prepared by swelling the cross-linked polymer with AgNO₃ aqueous solutions following γ-irradiation at 14 kGy·h⁻¹ dose rate, complete reduction of Ag(I) being achieved at 8 kGy (4 mM AgNO₃). Later on, the same group reported the poly(N-vinyl-2-pyrrolidone) (PVP)-AgNPs hydrogel nanocomposite preparation [30]. It was shown that PVP-AgNPs nanocomposites exhibited higher values of equilibrium swelling degree, Young's modulus, and molar mass between cross-links, while lower values of the diffusion coefficient and effective cross-link density were obtained, as compared to the pure PVP. Likewise, poly(HEMA) reported herein has excellent transparency, bio-compatibility (used in tissue engineering scaffolds, controlled drug delivery systems, wound dressings, etc.) and it has been originally used as a copolymer in contact lenses manufacturing providing suitable support for both optical and biomedical devices. Furthermore, copolymerization with MADQUAT, a monomer conferring thermally responsive solution properties to HEMA--based polymers and subsequent conversion of the hydrogel into a nanocomposite containing AuNPs has been evaluated for remote-controlled drug delivery based on hydrogel collapse at temperatures above lower critical solution temperature (LCST) resulting in a burst release of drugs.

This note reports on preliminary results on the radiolytic synthesis of gold nanocomposites within two types of hydrogels based on HEMA: (i) plain poly(HEMA) networks with various contents in ethylene glycol dimethacrylate (EGDMA) as a cross-

-linker and (ii) stimuli-responsive (SR) networks prepared from the same monomers copolymerized with [2-(methacryloyloxy)ethyl]trimethylammonium chloride (MADQUAT), which is expected to impart a pH-dependent behaviour to the resulting copolymer network. These approaches require an advanced control of chemical modifications at the different stages of the elaboration process.

The synthesis of the host matrices was achieved by photopolymerization using UV radiation, a versatile method that allows for the rapid formation of hydrogel materials in various dimensions and shapes. We have also shown that, besides the gels mentioned above, other poly(HEMA)-based stimuli-sensitive gels can be easily obtained by this approach, including pH-sensitive gels containing acrylic acid (AA) and temperature-sensitive gels containing N-isopropylacrylamide (NIPAm).

The obtained poly(HEMA)-based materials were characterized to assess the properties of the hydrogels, in the as-prepared state, after purification, and after EB-irradiation under various conditions. Attention was particularly paid to isothermal swelling in aqueous media.

In-situ formation of AuNPs was achieved by radiation-induced reduction of Au(III) ions present in the liquid phase of the hydrogels. UV-visible spectroscopy was selected as a simple and quite informative means for measuring the extent of the reductive process and for assessing some features of the formed nanoparticles. Preliminary tests were performed to evaluate the relevance of this method to pattern and to fix nanocomposite images in the depth of the hydrogel substrates.

Experimental

Chemicals

2-Hydroxyethyl methacrylate (97%), EGDMA (98%), 2-hydroxy-2-methylpropiophenone (>96%), 2-hydroxy-2-methyl-1-phenyl-1-propanone (Darocur 1173), hydrogen tetrachloroaurate trihydrate (99.99%), 2-(MADQUAT (75% aqueous solution), and N-isopropylacrylamide (≥99%) were purchased from Merck-Sigma-Aldrich, while AA (98%) was supplied by Acros Organics. The monomers were used as received. 2-Propanol (99.6%) was provided by VWR (Poland) and hydrogen peroxide (30% in water) by Chempur (Poland). Aqueous solutions and swelling media were prepared using double distilled water.

Synthesis of poly(HEMA) xerogels

The polymerization of HEMA monomer with EGDMA as cross-linker and Darocur 1173 as photoinitiator was performed in bulk. Approximately 1.5 g of a precursor mixture based on HEMA, EGDMA, and Darocur 1173 (99.0 wt%, 0.5 wt% and 0.5 wt%, respectively, which correspond to 8.192 M for methacrylate functions and 0.033 M for the photoinitiator)

was poured into a poly(tetrafluoroethylene) (PTFE) mold and exposed in air to the fluorescent tubes emitting at 365 nm for 15 min with an irradiance of 6 mW·cm^{-2} (UV Biolink, Vilber-Lourmat). The surface of the cured poly(HEMA) disks was washed with isopropanol, the disk samples were dried to constant weight in an oven at 60°C, and finally polished to obtain a uniform thickness of 1.0 ± 0.05 mm.

Synthesis of neat and stimuli-sensitive hydrogels based on poly(HEMA) in aqueous solutions

In this procedure, cross-linking polymerization was performed in concentrated aqueous solutions of monomers containing hydrogen peroxide as a co-initiator. Gels based on pure poly(HEMA) have been synthesized at a constant ratio of HEMA to EGDMA equal 99:1 (v/v); this solution has been mixed with 30% aqueous solutions of H_2O_2 at volume ratios of 1:1, 2:1, 3:1, and 4:1. After homogenization, 1 ml of the final solution has been poured into the PTFE mold, resulting in a liquid layer thickness of 2 mm, and exposed to the air to 254 nm photon beam with an irradiance of 2.6 mW·cm^{-2} (CL-1000 Ultraviolet Crosslinker, UVP) at total exposure doses up to 22 J·cm^{-2}.

Gels containing MADQUAT have been synthesized by UV irradiation (as above, exposure dose kept constant at 8 J·cm^{-2}) of solutions containing 50 vol.% of aqueous 30% H_2O_2, 45–48.75 vol.% of HEMA/EGDMA (99:1) solution, and 1.25–5 vol.% of aqueous 75% MADQUAT, with no pH adjustment. Gels containing AA or N-isopropylacrylamide (NIPAm) have been synthesized by the same method, using solutions containing from 1.25 vol.% to 5 vol.% AA or NIPAm. Molar compositions of all samples used for synthesizing hydrogels in aqueous systems are shown in Tables 1–4.

For swelling tests of MADQUAT- or AA-containing gels, pH was adjusted with 1 M solutions of NaOH or HCl, and swelling was performed at room temperature (RT). Swelling tests of NIPAm-containing gels have been performed in water (no pH adjustment), in beakers placed in a temperature-controlled bath.

Electron beam irradiation and *in situ* synthesis of AuNPs

Irradiation of the poly(HEMA)-based materials was performed with a 10 MeV Linac at an average dose rate of about 3 kGy·s^{-1} (IONISOS, Chaumesnil, France). The treatment was fractionated in 5 kGy-passes for doses up to 20 kGy, and in 25 kGy-passes for doses from 25 kGy to 100 kGy. Poly(HEMA) samples in water-swollen or dry states were sealed in plastic bags with a minimum amount of air and submitted to EB-irradiation at doses up to 100 kGy. Radiolytic synthesis of poly(HEMA)-AuNPs composites was performed on poly(HEMA) disks swollen with Au(III) aqueous solution. The samples sealed in plastic bags with a minimum amount of air and kept

Table 1. Gelation dose (D_g) and probability ratio of chain breakage to cross-linking (p_0/q_0) for hydrogels based on HEMA/EGDMA with the addition of a different amount of H_2O_2 (30% aqueous solution) synthesized by UV irradiation (254 nm, irradiance 2.6 mW·cm^{-2})

Sample make-up	HEMA/EGDMA (99/1): 50 vol.% 30% H_2O_2: 50 vol.%	HEMA/EGDMA (99/1): 67 vol.% 30% H_2O_2: 33 vol.%	HEMA/EGDMA (99/1): 75 vol.% 30% H_2O_2: 25 vol.%	HEMA/EGDMA (99/1): 80 vol.% 30% H_2O_2: 20 vol.%
Sample composition	methacrylate functions 4.123 mol·L^{-1} H_2O_2 4.895 mol·L^{-1}	methacrylate functions 5.497 mol·L^{-1} H_2O_2 3.263 mol·L^{-1}	methacrylate functions 6.184 mol·L^{-1} H_2O_2 2.448 mol·L^{-1}	methacrylate functions 6.596 mol·L^{-1} H_2O_2 1.958 mol·L^{-1}
D_g (J·cm^{-2})	2.33	2.55	2.92	3.55
p_0/q_0	0	0	0	0.25

Table 2. Gel fractions for hydrogels based on HEMA/EGDMA/H_2O_2 (30% aqueous solution) with various amounts of MADQUAT (75% aqueous solution), synthesized by UV irradiation (254 nm, irradiance 2.6 mW·cm^{-2}, total exposure dose 8 J·cm^{-2})

Sample make-up	HEMA/EGDMA (99/1): 50 vol.% 30% H_2O_2: 50 vol.%	HEMA/EGDMA (99/1): 48.75 vol.% MADQUAT 1.25 vol.% 30% H_2O_2: 50 vol.%	HEMA/EGDMA (99/1): 47.5 vol.% MADQUAT 2.5.% 30% H_2O_2: 50 vol.%	HEMA/EGDMA (99/1): 45 vol.% MADQUAT 5 vol.% 30% H_2O_2: 50 vol.%
Sample composition	methacrylate functions 4.123 mol·L^{-1} H_2O_2 4.895 mol·L^{-1}	methacrylate functions 4.020 mol·L^{-1} MADQUAT 0.049 mol·L^{-1} H_2O_2 4.895 mol·L^{-1}	methacrylate functions 3.917 mol·L^{-1} MADQUAT 0.097 mol·L^{-1} H_2O_2 4.895 mol·L^{-1}	methacrylate functions 3.710 mol·L^{-1} MADQUAT 0.194 mol·L^{-1} H_2O_2 4.895 mol·L^{-1}
Gel fraction (%)	82.0	75.1	65.3	50.9

Table 3. Gel fractions for hydrogels based on HEMA/EGDMA/H_2O_2 (30% aqueous solution) with various amounts of AA, synthesized by UV irradiation (254 nm, irradiance 2.6 mW·cm^{-2}, total exposure dose 8 J·cm^{-2})

| Sample make-up	HEMA/EGDMA (99/1): 50 vol.% 30% H_2O_2: 50 vol.%	HEMA/EGDMA (99/1): 48.75 vol.% AA: 1.25 vol.% 30% H_2O_2: 50 vol.%	HEMA/EGDMA (99/1): 47.5 vol.% AA: 2.5 vol.% 30% H_2O_2: 50 vol.%	HEMA/EGDMA (99/1): 45 vol.% AA: 5 vol.% 30% H_2O_2: 50 vol.%
Sample composition	methacrylate functions 4.123 mol·L^{-1} H_2O_2 4.895 mol·L^{-1}	methacrylate functions 4.020 mol·L^{-1} AA 0.182 mol·L^{-1} H_2O_2 4.895 mol·L^{-1}	methacrylate functions 3.917 mol·L^{-1} AA 0.364 mol·L^{-1} H_2O_2 4.895 mol·L^{-1}	methacrylate functions 3.710 mol·L^{-1} AA 0.729 mol·L^{-1} H_2O_2 4.895 mol·L^{-1}
Gel fraction (%)	82.0	92.2	90.9	88.3

Table 4. Gel fractions for hydrogels based on HEMA/EGDMA/H_2O_2 (30% aqueous solution) with various amounts of *N*-isopropylacrylamide, synthesized by UV irradiation (254 nm, irradiance 2.6 mW·cm^{-2}, total exposure dose 8 J·cm^{-2})

Sample make-up	HEMA/EGDMA (99/1): 50 vol.% 30% H_2O_2: 50 vol.%	HEMA/EGDMA (99/1): 48.75 vol.% NIPAm: 1.25 wt% 30% H_2O_2: 50 vol.%	HEMA/EGDMA (99/1): 47.5 vol.% NIPAm: 2.5 wt% 30% H_2O_2: 50 vol.%	HEMA/EGDMA (99/1): 45 vol.% NIPAm: 5 wt% 30% H_2O_2: 50 vol.%
Sample composition	methacrylate functions 4.123 mol·L^{-1} H_2O_2 4.895 mol·L^{-1}	methacrylate functions 4.020 mol·L^{-1} NIPAm 0.110 mol·L^{-1} H_2O_2 4.895 mol·L^{-1}	methacrylate functions 3.917 mol·L^{-1} NIPAm 0.221 mol·L^{-1} H_2O_2 4.895 mol·L^{-1}	methacrylate functions 3.710 mol·L^{-1} NIPAm 0.442 mol·L^{-1} H_2O_2 4.895 mol·L^{-1}
Gel fraction (%)	82.0	75.8	70.3	65.7

in the dark before being submitted to EB-irradiation at doses from 5 kGy to 25 kGy.

Synthesis of AuNPs in the poly(HEMA-co--MADQUAT) hydrogels has been performed by swelling gel samples (synthesized as described above and pre-swollen in water for two weeks) in freshly made aqueous 1 mM Au(III) solution at pH 2 or pH 7 for 2 h, and subsequent immediate irradiation by 6 MeV electron beam (EB) generated by Elektronika ELU-6e linear accelerator (pulsed beam, 20 Hz, 4 µs pulse duration, the average dose rate of 63 Gy·s^{-1} as determined by polymer film dosimetry – B3WIN-
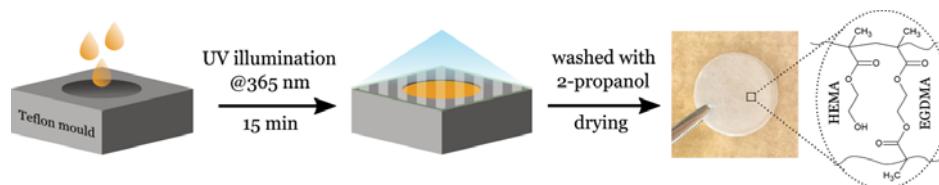
Scheme 1. Scheme of the poly(HEMA) xerogel synthesis by photopolymerization.

-Dose Dosimeters by GEX Corporation USA) at a total dose of 1 kGy, 2 kGy, and 5 kGy, in closed but not sealed Petri dishes.

Swelling measurements

Structural changes occurring in poly(HEMA) networks upon exposure to EB were evaluated by swelling measurements. The swollen hydrogels were removed from flasks filled with double distilled water at regular time intervals, blotted with a clean paper towel, weighed, and replaced in the same soaking water bath. The swelling measurements were continued until a constant weight was reached for each sample. All measurements were made in duplicate. The equilibrium degree of swelling (DS_{eq}) was calculated from the difference in weight between the disk's weight in the equilibrium swollen state w_{eq} at 30°C and as material dried to constant weight w_0, using Eq. (1).

$$(1) \qquad DS = \frac{w_{eq} - w_0}{w_0}$$

The final weight loss from the extractables after EB irradiation was estimated using Eq. (2),

$$(2) \qquad \text{weight loss (\%)} = \frac{w_0 - w_{irr}}{w_0} \times 100\%$$

where w_0 is the initial weight of dry disk before irradiation, w_{irr} is the weight of the irradiated disk (in the swollen or dried state), swollen to extract possible scission fragments and dried to constant weight.

Alternatively, the degree to which the monomer and cross-linker have been polymerized and incorporated into the covalent network can be expressed as the gel fraction (Eq. (3)).

$$(3) \qquad \text{gel fraction (\%)} = 100\% - \text{weight loss (\%)}$$

Spectroscopic and thermomechanical analysis (DMA) of poly(HEMA) materials

DMA measurement was performed on non-irradiated and EB-treated 1 mm-thick poly(HEMA) bars to measure the viscoelastic response using a Q800 DMA rheometer (TA Instruments) at 1 Hz frequency and 15 μm amplitude in the temperature interval from 30°C to 180°C.

The spectroscopic properties of polished poly(HEMA) substrates and nanocomposites were recorded in the UV-vis domain (transmission mode, from 200 nm to 800 nm) with an Agilent Cary 50 instrument (Agilent Technologies, Santa Clara, CA, USA).

Results and discussion

Photochemical synthesis of PHEMA-based xerogels

Free radical polymerization of blends including HEMA as the main monomer (99.5, 99.4, 99.0, 98.5 or 94.5 wt%), EGDMA as a cross-linking agent (0, 0.1, 0.5, 1 or 5 wt%), and Darocur 1173 as the photoinitiator (0.5 wt%) was carried out upon exposure to 365 nm resulting in the formation of cross-linked hydrophilic networks as illustrated in Scheme 1.

The choice of the photoinitiator and its concentration in the blend has been made in such a way that the incident beam 365 nm penetrates deeply into the 1.5 mm thick samples, due to the low absorption coefficient of the photoinitiator's n-π* transition. Simple calculations showed that under these experimental conditions the gradient of energy absorption between the top and bottom surfaces of the sample is very limited [24].

FTIR monitoring

To monitor the progress of HEMA polymerization, Fourier-transform infrared spectroscopy (FTIR) measurements were performed on 2 mm-thick samples of HEMA/EGDMA/Darocur 1173 (99/0.5/0.5 wt%) precursor mixture cured by exposure to the 365 nm source for cumulated time intervals. As seen from Fig. 1, the near IR band at 6168 cm^{-1}, corresponding to the third harmonic wavenumber of the methacrylate C=C double bond stretching mode, is gradually decreasing as the exposure to UV illumination increases from 0 min to 60 min.

Kinetic profiles representing the progress of methacrylate polymerization in monomer blends con-
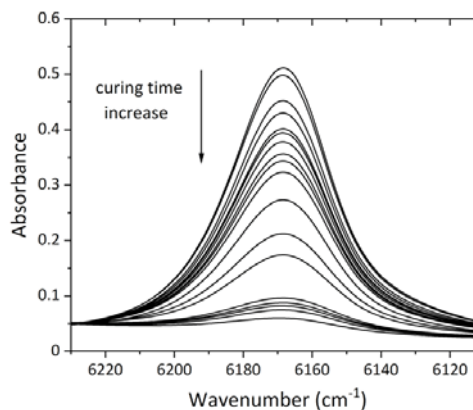

Fig. 1. Evolution of the near IR band assigned to methacrylate $\nu CH_2=C<$ groups as a function of UV curing time (0–60 min) for a 2 mm-thick sample based on HEMA/EGDMA/Darocur 1173 (99/0.5/0.5 wt%).
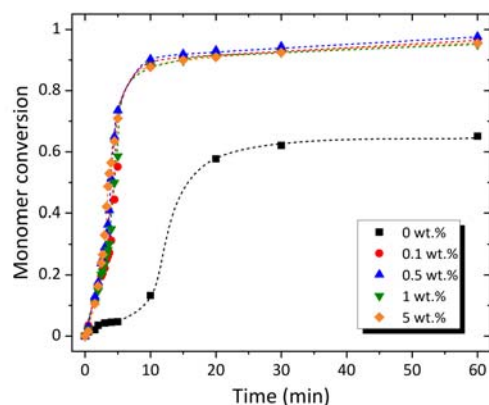
Fig. 2. Monomer conversion as a function of curing time for HEMA/EGDMA/Darocur 1173 at various EGDMA content (0, 0.1, 0.5, 1, and 5 wt%) and constant Darocur 1173 concentration of 0.5 wt%.

taining various amounts of EGDMA (0, 0.1, 1, and 5 wt%) were obtained using this method, monomer conversion being calculated from Eq. (4),

$$(4) \qquad X = 1 - \frac{A_t}{A_0}$$

where A_t is the measured absorbance at time t, and A_0 is the absorbance before starting irradiation.

The kinetic profile recorded for HEMA polymerization in absence of any cross-linker has the typical sigmoidal shape observed for the bulk polymerization of methyl methacrylate [31], initially with a slow rate and an auto-acceleration stage, well-documented as the Trommsdorff effect [32, 33], which develops at about 10% of monomer conversion, as a consequence of drastic decrease in bimolecular termination rate constant in the viscous medium, and then levels off to reach a final conversion of 60–65% in the vitrified material (Fig. 2). For monomer blends with EGDMA content as low as 0.1 wt%, polymerization proceeds much faster and exhibits a change to another auto-accelerated regime when the conversion level reaches 30–35%. Several experiments conducted with EGDMA concentrations between 0.5 wt% and 5 wt% showed almost the same profile, with a conversion of 90% reached within 10 min, and a very slow completion of the reaction between 10 min and 60 min of exposure.

From a practical perspective, it was found convenient to produce the xerogels with various contents of cross-linking agent cured by photoirradiation for 15 min.

Photochemical synthesis of neat and SR hydrogels

UV irradiation (254 nm) of concentrated aqueous solutions of HEMA/EGDMA containing hydrogen peroxide as a co-initiator resulted in the formation of permanently cross-linked hydrogels. While this procedure requires high hydrogen peroxide content in the reagent mixture, it is an efficient way of synthesizing poly(HEMA) hydrogels. Gel fractions as a function of exposure dose for various monomer/aqueous 30% H_2O_2 ratios are shown in Fig. 3.
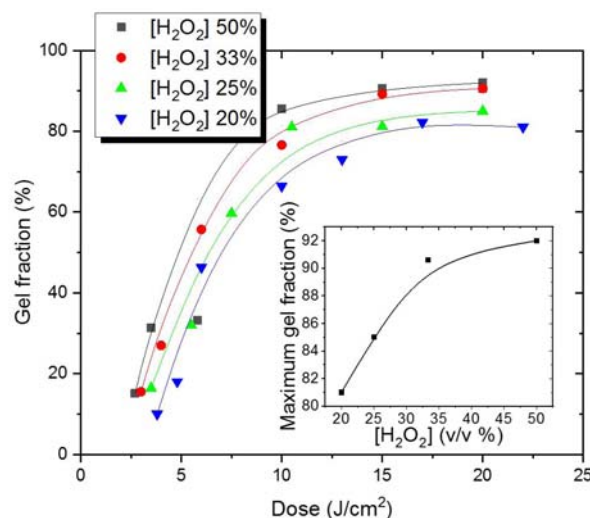

Fig. 3. Gel fraction as a function of exposure dose in synthesizing poly(HEMA) hydrogels by UV irradiation (254 nm, irradiance 2.6 mW·cm⁻²) of concentrated aqueous monomer/cross-linker solution containing hydrogen peroxide. Volume fractions of aqueous 30% H_2O_2 solutions are given in the graph, the remaining fraction being 99/1 v/v HEMA/EGDMA. Inset: maximum gel fraction as a function of hydrogen peroxide content (as the volume fraction of aqueous 30% H_2O_2 solution).

It can be seen that, when this procedure is used, exposure doses necessary to reach considerable gel fraction (>80%) are in the range of 10–15 J·cm⁻², which is at least 2–3 times higher than in the case of xerogel synthesis described above. Moreover, the maximum gel content was somewhat lower than for the xerogels. It has been found that both the yield of gel formation and the final gel content depend to some extent on the sample composition. More efficient cross-linking and higher gel fractions were obtained for samples of higher H_2O_2/monomer ratios, albeit these dependencies were not much pronounced (11% increase in gel fraction achieved by more than doubling the peroxide content, see inset in Fig. 3). Another indication of hydrogen peroxide influence on the cross-linking process is the values of gelation doses, D_g, understood as the minimum exposure doses at which macroscopic gel appears in the system, calculated from data shown in Fig. 3 using the modified Charlesby–Pinner approach [34] (Table 1).

Gelation doses systematically decrease with the increasing H_2O_2 content, pointing out to more efficient cross-linking. These results indicate that the initiation process, rather than the subsequent cross-linking polymerization, is the decisive step governing the efficiency of hydrogel formation in this system.

Another parameter resulting from these calculations is the probability ratio of chain breakage to cross-linking, p_0/q_0. This ratio is zero (within the experimental error) for all hydrogen peroxide concentrations save the lowest one, pointing out that degradation of the formed chains and network is negligible except for low hydrogen peroxide content.

The swelling properties of the poly(HEMA) hydrogels obtained by this method depend on UV exposure dose, as is shown in Fig. 4.
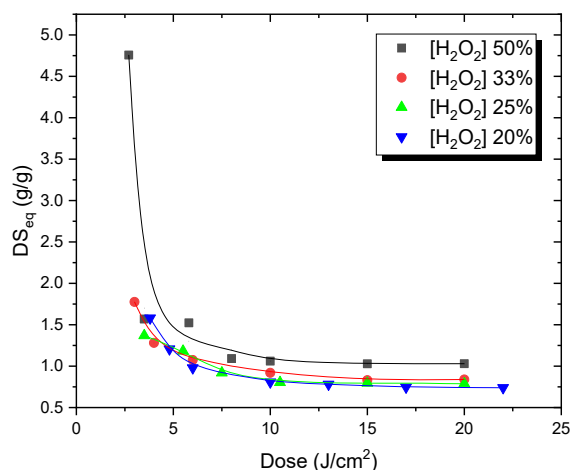
Fig. 4. Equilibrium degree of swelling of poly(HEMA) hydrogels synthesized by UV irradiation (254 nm, irradiance 2.6 mW·cm⁻²) of concentrated aqueous monomer/cross-linker solution containing hydrogen peroxide. Volume fractions of aqueous 30% H_2O_2 solutions are given in the graph, the remaining fraction being 99/1 v/v HEMA/EGDMA. Swelling tests performed in water at RT.

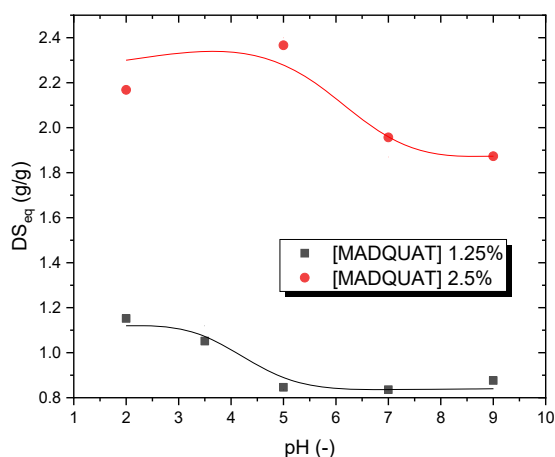**Fig. 5.** Equilibrium degree of swelling of poly(HEMA-co--MADQUAT) hydrogels synthesized by UV irradiation (254 nm, irradiance 2.6 mW·cm⁻², exposure dose 8 J·cm⁻²) of solutions composed of 50 vol.% of aqueous 30% hydrogen peroxide, 47.5–48.75 vol.% of HEMA/EGDMA (99/1) and 1.25–2.5 vol.% of aqueous 75% MADQUAT, as a function of pH.

As expected, the cross-link density increases with exposure dose, leading to a pronounced decrease in the equilibrium degree of swelling. At high doses, while monomer and cross-linker are nearly fully converted into a 3D network, the gels can adsorb ca. 0.8–1.2 g of water per gram of dry gel. While there is no pronounced difference in the swelling properties between the gels synthesized in the presence of 20–33% of hydrogen peroxide solution (and 67–80% of monomer/cross-linker mixture), products based on irradiation of samples containing 50% of H_2O_2 solution (and 50% of HEMA/EGDMA) have somewhat higher tendency to swell. This indicates that solutions irradiated at relatively low monomer and cross-linker concentrations formed somewhat less densely cross-linked networks.

Based on the above-described synthetic procedure, three kinds of stimuli-sensitive hydrogels have been synthesized, where HEMA/EGDMA has been polymerized and cross-linked in the presence of MADQUAT or AA to render pH-responsive properties or *N*-isopropylacrylamide to yield temperature--sensitive products, respectively. The exposure dose for these samples has been set at 8 J·cm⁻² and the volume fraction of aqueous 30% hydrogen peroxide was constant at 50%. Samples contained 45–48.75 vol.% of HEMA/EGDMA (99:1) and 1.25–5 vol.% of one of the above-listed monomers (or its 75% aqueous solution in the case of MADQUAT).

The influence of MADQUAT content on the gel fraction is shown in Table 2.

Increasing the MADQUAT fraction has a clear negative effect on the efficiency of gel formation. This can be traced down to the positive charge on the monomer, which causes electrostatic repulsion between the growing polymer chains and the monomer, and also to the scavenging of ·OH radicals resulting from photolysis of hydrogen peroxide by chloride ions, a very efficient reaction ($k = 4.3 \times 10^9$ dm³·mol⁻¹·s⁻¹ [35]). Nevertheless, at MADQUAT concentrations up to 2.5 vol.% of its 75% solution, stable gels of

reasonable mechanical properties are obtained. Their behaviour in water at various pH is shown in Fig. 5.

In the whole range of tested pH, the equilibrium degree of swelling is significantly higher for the gel synthesized with higher MADQUAT contents. This can be traced down to two effects – lower cross-link density due to less efficient cross-linking polymerization and also higher hydrophilicity of the network due to the higher content of highly hydrophilic MADQUAT. Both synthesized gels show some response to pH, with the transition located in the pH range of 4–6.

The method can also be applied for synthesizing hydrogels containing AA. The efficiency of gel formation is in this case significantly higher than for MADQUAT. Interestingly, the addition of 1.25% of AA to the HEMA/EGDMA solution in water/H_2O_2 seems to increase the gel fraction (Table 3), which might be related to hydrogen bond formation between the growing poly(HEMA) chains and protonated AA, an effect potentially facilitating polymerization. Only when higher amounts of AA are added, some decrease in the cross-linking yield is observed. The obtained gels are strongly sensitive to pH (Fig. 6).

At low pH, most of the carboxylic groups are protonated. There is no charge along the chain, thus no repulsive forces act between the segments, and also hydroxyl groups of HEMA may form hydrogen bonds with protonated carboxylic groups. Therefore the swelling ability of the gel is moderate. However, at pH >5, deprotonation of carboxylic groups leads to the formation of ionic groups and an increase of linear charge density along the chains. High hydrophilicity and electrostatic repulsion between the charged chain segments lead to strong expansion and swelling. The equilibrium degree of swelling at neutral and high pH depends on the content of AA in the initial mixture. While for 1.25% of AA it levels off at ca. 9 g·g⁻¹, for higher AA content it reaches over 30 g·g⁻¹ at pH 9. Such pronounced pH

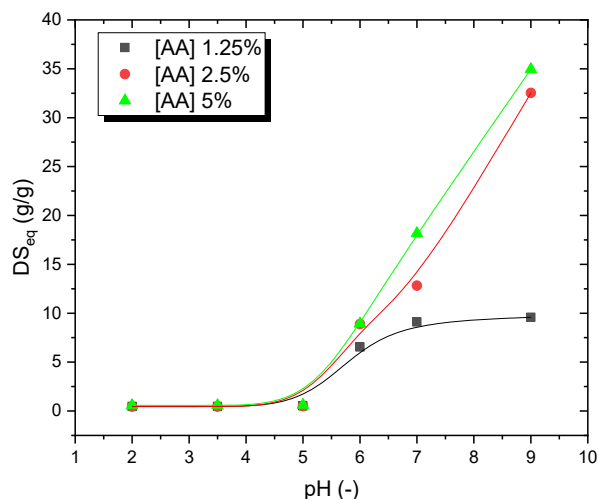**Fig. 6.** Equilibrium degree of swelling of poly(HEMA-co--AA) hydrogels synthesized by UV irradiation (254 nm, irradiance 2.6 mW·cm^{-2}, exposure dose 8 J·cm^{-2}) of solutions composed of 50 vol.% of aqueous 30% hydrogen peroxide, 45–48.75 vol.% of HEMA/EGDMA (99/1) and 1.25–5 vol.% of AA, as a function of pH.

effects are known from studies on neat poly(AA) hydrogels [36]. It is expected that the average pK_a of carboxylic groups in the studied copolymer gels is between the values for the low-molecular-weight analog, i.e. propionic acid (pK_a = 4.9 [37]) and for poly(AA) (average p$K_a \approx$ 6 [38]). Comparing these values to the data shown in Fig. 6 indicates that in the obtained gels more than half of the carboxylic groups must be dissociated for a strong increase in swelling capacity to be observed.

Gel fractions obtained by UV-irradiation of samples containing 1.25–5 vol.% of NIPAm (50 vol.% of 30% aqueous hydrogen peroxide, 45–48.75 vol.% of HEMA/EGDMA (99/1)) are shown in Table 4, while Fig. 7 illustrates equilibrium degree of swelling for NIPAm-containing hydrogels as a function of temperature.
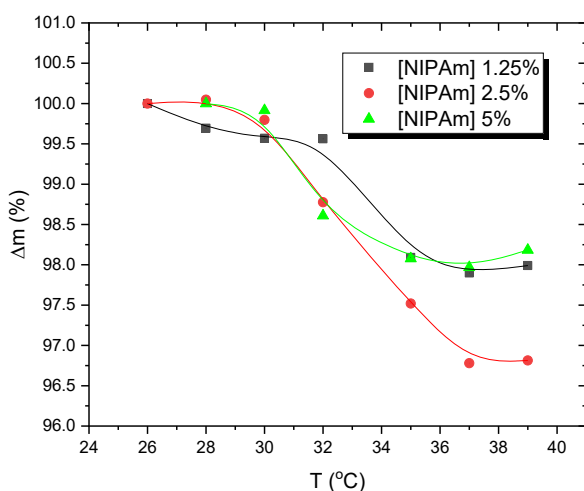

Fig. 7. Weight at equilibrium swelling of poly(HEMA--co-NIPAm) hydrogels synthesized by UV irradiation (254 nm, irradiance 2.6 mW·cm^{-2}, absorbed dose 8 J·cm^{-2}) of solutions composed of 50 vol.% of aqueous 30% hydrogen peroxide, 45–48.75 vol.% of HEMA/EGDMA (99/1) and 1.25–5 vol.% of NIPAm, as a function of temperature, normalized to the weight at equilibrium swelling at 26.0°C.

While NIPAm content in the studied systems was relatively low, the products do exhibit some responsiveness to temperature. The observed mild but clear changes occur at a transition temperature of ca. 32–34°C, which agrees well with the LCST of poly(NIPAm) in water [39]. Interestingly, the highest amplitude of changes in equilibrium degree of swelling was observed for hydrogels based on samples of 2.5 vol.% of NIPAm, i.e., the medium NIPAm content within the used range.

Swelling properties of xerogels modified by ionizing radiation

Polymers exposed to ionizing irradiation generally undergo competing cross-linking and chain scission (degradation) processes, yielding final properties of the material that depend critically on the balance between these two main reaction pathways. Methacrylate polymers, particularly PMMA, are known to be sensitive to the direct effect of ionizing radiation and primarily degrade through main chain scission [40, 41]. However, due to the presence of functional side-groups, particularly when water is present inside the polymer matrix (i.e. hydrogels), one can expect that the products of water radiolysis, namely e$^-_{aq}$ and strongly oxidizing hydroxyl radicals $^{\cdot}$OH, may promote reactions of hydroxyethyl ester lateral chains, which may result in intrachain bridges and intermolecular cross-links.

Therefore, to investigate the radiation-induced changes occurring in the water-swollen poly(HEMA) network, hydrogel disks were exposed to 10 MeV EB irradiation at doses varied between 5 kGy and 100 kGy. Before EB irradiation, the disks were equilibrated in pure water and dried of total three times to eliminate the non-reacted compounds during photo--polymerization from the xerogels. After irradiation, the same washing protocol has been applied to leach out the products of polymer radiolysis. All disks have been dried to constant weight before swelling measurements. To assess the radiation-induced changes in our system, the diffusion coefficients were calculated following the formalism of the second Fick's law, considering an unsteady one-dimensional diffusion under isothermal conditions. For a short-time approximation, a solution of Fick's second law for a plane sheet of thickness l can be expressed by Eq. (5),

$$(5) \qquad \frac{m_t}{m_\infty} = \frac{4}{l}\left(\frac{Dt}{\pi}\right)^{1/2}$$

where m_t is the mass of the swollen sample at time t, m_∞ is the equilibrium mass, and l is the thickness of the studied disk. From the latter, for Fickian diffusion, one can express diffusion coefficient D which is proportional to the square of the slope, β, according to Eq. (6) [42].

$$(6) \qquad D = \frac{\pi l^2 \beta^2}{16}$$

Figure 8 depicts swelling kinetic profiles of poly(HEMA) hydrogels irradiated at various doses as compared to non-irradiated ones which follow
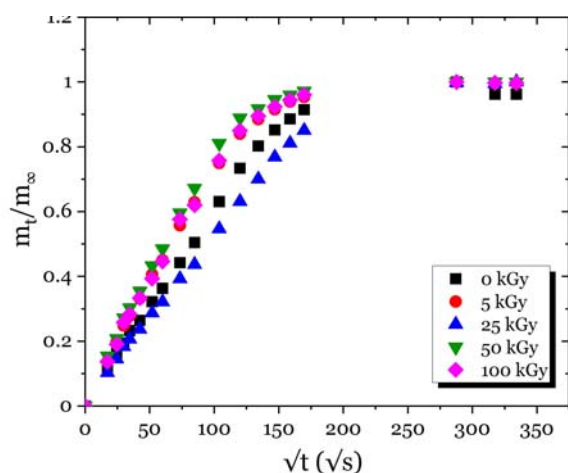
Fig. 8. Effect of irradiation dose (0–100 kGy) applied to the water-swollen hydrogels on their swelling kinetic profiles of the corresponding dried xerogels soaked in water at 30°C.

Fig. 9. Plots of thermomechanical dissipation factor tan δ against temperature in DMA measured for poly(HEMA) hydrogels EB irradiated at 5–100 kGy. Measurement parameters: 1 Hz frequency and 15 μm amplitude in the temperature interval from 30°C to 180°C.

Fickian type diffusion (n = 0.5). There was only a slight variation of the diffusion coefficient with dose observed – D increases from 1.40 to 1.75 $\times$ 10^{-11} m$^2 \cdot$s^{-1} as the dose was increased from 0 to 100 kGy, respectively. In contrast with this increase of the diffusion coefficient for irradiated poly(HEMA) hydrogels, the weight loss measured after extensive desorption of the soluble components in water was found to be somewhat smaller than that of polymer EB-irradiated in the dry state (2.90% and 6.2% at 100 kGy, respectively). Furthermore, the equilibrium degree of swelling of these gels remained virtually independent on the dose.

It can be suggested therefore that EB irradiation (<100 kGy) seems to induce cross-linking in hydrogels while xerogels primarily tend to degrade with a higher weight loss supported by larger amounts of extractables. At the same time, it has little effect on the polymer network. It is worth mentioning that as far as bulk photopolymerization is used, network formation under non-equilibrium conditions can also result in uncontrolled defects within the network, hence inducing some variability in the obtained results.

DMA is another sensitive technique for investigating the changes in the dynamics of polymer chains in a network over large temperature ranges. Figure 9 shows the very small evolution of the dissipation factor tan δ recorded by thermomechanical analysis of poly(HEMA) networks irradiated in the equilibrium water-swollen state. The glass transition temperature T_g seems to vary very slightly, by only a few degrees (from 124.4°C before irradiation to 126.1°C after 50 kGy), while the tan δ_{max} value decreases smoothly from 0.92 to 0.86 in the same dose interval. These two observations can be interpreted by a limited loss in mobility for the macromolecular chains upon irradiation, as a consequence of a reduction of free volume and an increase in cross-link density with dose.

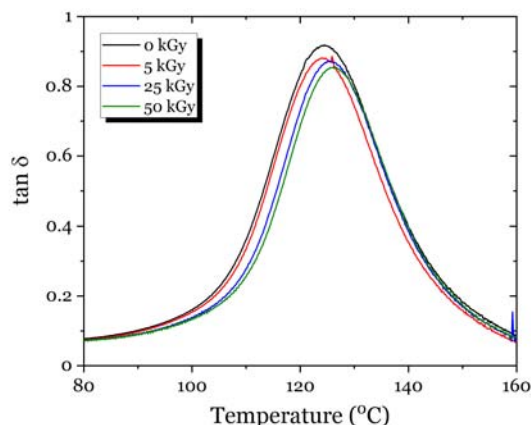These results obtained by assessing transport and thermophysical properties of irradiated poly(HEMA) networks neither reveal a strong trend towards chain scission nor a dominant increase in cross-linking density upon EB irradiation of the swollen hydrogels. This suggests that both processes seem to balance each other out. A deeper investigation with quantitative measurements of the effects of radiation on linear poly(HEMA) would allow to ascertain these preliminary conclusions. Concerning our main objective consisting in the formation of AuNPs within the hydrogels, the limited effects on the poly(HEMA) matrix observed at doses below 15–20 kGy provides an interesting processing window for the radiolytic reduction of Au(III) ions with minimal impact on the properties of the host polymer.

In-situ radiolytic reduction of Au(III) salts within swollen hydrogels

To produce nanocomposites, poly(HEMA) disks were equilibrated in 1 mM Au(III) aqueous solutions, sealed in plastic bags (under air), and stored in dark before EB irradiation. No radical scavenger was used at this stage of the study. Preliminary experiments showed that the xerogel samples, when used as prepared by photopolymerization, were able to form AuNPs upon Au(III) sorption, likely due to the presence of occluded reducing species within the vitrified matrix. This undesirable effect was suppressed by pre-swelling the material in water and drying which may result either in relaxation and quenching of trapped reactive species or desorption of reductive compounds.

After pre-washing, Au(III) loaded hydrogel disks were found chemically inert concerning the guest ions and were suitable for studying the effect of an EB treatment at doses varied from 5 kGy to 25 kGy. Upon irradiation, the initially pale yellow-coloured disks turned dark pink, exhibiting an absorption band at ca. 550 nm which is a characteristic feature of surface plasmon resonance (SPR) of AuNPs.

First, hydrogels soaked in 1 mM Au(III) were EB irradiated at doses of 0–25 kGy. A slight blue shifting and narrowing of the SPR band by increasing the
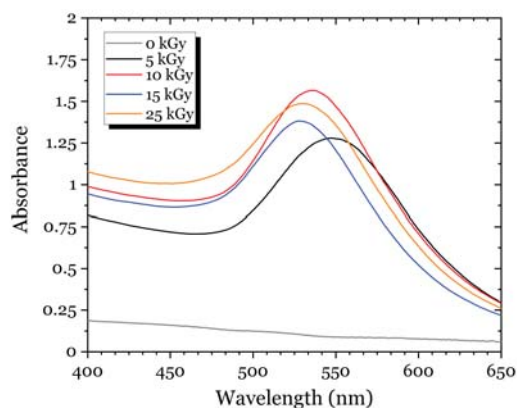
Fig. 10. Effect of EB dose on the visible absorption spectrum of poly(HEMA)-AuNPs composite disks (1 mm-thick, soaked in 1 mM Au(III)).
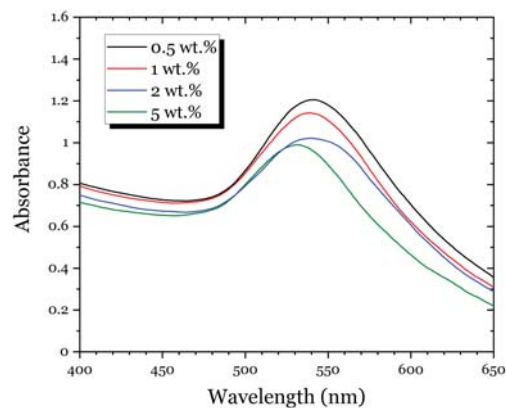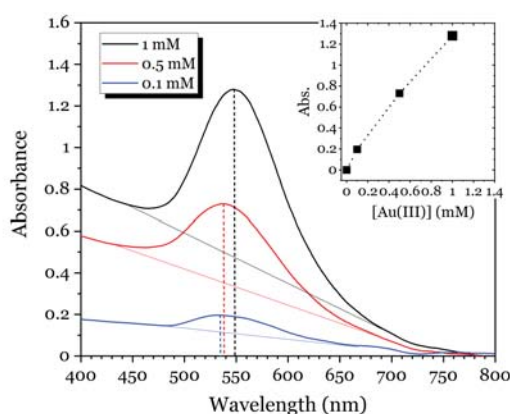

Fig. 11. Radiolytic formation of AuNPs within poly(HEMA) matrix upon EB irradiation of 1 mM, 0.5 mM, and 0.1 mM Au(III) loaded hydrogels at 5 kGy. Inset: Absorbance as a function of Au(III) concentration.

absorbed dose of radiation (Fig. 10) were observed, indicating a smaller NP size.

Figure 11 depicts UV-vis spectra of poly(HEMA)-AuNPs hydrogel composites equilibrated in Au(III) aqueous solutions of various concentrations before irradiation. As seen from the inset in Fig. 11, the SPR band is increasing monotonically and almost proportionally with increasing of Au(III) concentration, confirming the fact that a 5 kGy dose might not be sufficient whilst a 10 kGy treatment would completely reduce absorbed gold ions.

Figure 12 illustrates the influence of EGDMA content (0.5, 1, 2, and 5 wt%) on the SPR absorption band of poly(HEMA)-AuNPs composites. The resonance band is shifted from 540 nm to 531 nm as the EGDMA content is increased, suggesting the formation of smaller particles with a narrower size distribution. Assuming that the poly(HEMA) networks have a uniform structure, increasing EGDMA concentration results in a higher cross-linking density, with a decrease in the elastic properties of the poly(HEMA) segments. This would expectedly affect the diffusion of reactive species and limit the growth of the metal nanoparticles.

Two different approaches were explored to synthesize AuNPs in a limited area, either by direct Au(III) reduction within the matrix at various

Fig. 12. Radiolytic formation of AuNPs within poly(HEMA) matrix upon EB irradiation of 1 mM Au(III) loaded hydrogels at 5 kGy with various EGDMA content.

doses or by pre-irradiation of dry or water-swollen disks followed by soaking in Au(III) solutions. To test the two approaches, lead masks were used to spatially control the irradiated areas in samples exposed to 10 MeV EB at 5 kGy. The typical colour change to purple-red assigned to the presence of AuNPs was precisely localized in irradiated areas of Au(III)-swollen hydrogels and not around (Fig. 13a). Furthermore, pre-irradiation of water-swollen disks and subsequent soaking in Au(III) solution resulted in a well-defined coloured spot, yet much smaller in intensity (Fig. 13b). To improve the latter approach, one needs to characterize and quantify the long-lived polymeric species responsible for Au(III) reduction. Based on these results, radiolytic post-modification of 2D and 3D poly(HEMA)-based patterns are envisioned as a promising fabrication method to generate nanocomposites with unique optical and sensing properties.

Radiation-induced formation of gold nanoparticles has also been performed in the poly(HEMA-MADQUAT) gels. Hydrogels obtained by UV irradiation (254 nm, irradiance 2.6 mW·cm^{-2}, exposure dose 8 J·cm^{-2}) of a solution composed of 50 vol.% of aqueous 30% hydrogen peroxide, 47.5 vol.% of HEMA/EGDMA (99/1) and 2.5 vol.% of aqueous 75% MADQUAT, after careful washing and swelling in water for two weeks, have been soaked in aqueous 1 mM Au(III) solutions of pH 2 and pH 7 for 2 h. Subsequently, they were surface-dried to remove excess liquid, placed in Petri dishes, and irradiated with the access of air by a beam of 6 MeV electrons from a linear accelerator with doses up to 5 kGy.
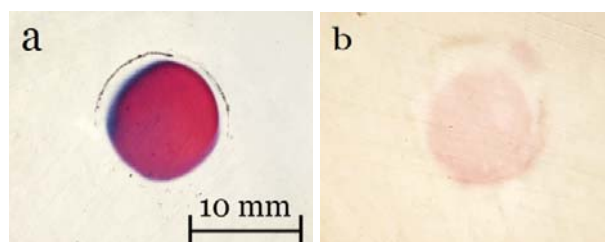

Fig. 13. Formation of AuNPs in a limited area exposed to EB of 5 kGy within poly(HEMA) disks (a) swollen in 1 mM Au(III) before irradiation and (b) post-swollen in 1 mM Au(III).

The formation of AuNPs is evidenced by the formation of distinct violet colour, especially in samples irradiated at pH 7 (Fig. 14). Soaking the composite gel in water for 24 h does not lead to any noticeable leaching of AuNPs from the gel matrix.

The apparent lack of AuNPs formation at 2 kGy is most probably caused by the oxygen content within the gels. The reducing species formed upon irradiation, e^-_{aq} and $H^\bullet$, had been initially strongly scavenged by oxygen until its concentration dropped to the level where the competing reactions of these transients, i.e., reduction of Au(III), started to dominate, yielding gold nanoparticles. The latter process is expected to be the main reaction channel for nanoparticle formation in our system, while we do not exclude some contribution of the α-hydroxyalkyl radicals formed by $^\bullet OH$ attack on the HEMA-based network. Radicals of this structure are known to be of reducing character, but their yield in our system and their reaction rate constant with Au(III) is expected to be much lower than corresponding values for e^-_{aq} and $H^\bullet$.

While there can be several reasons for the apparent lower yield of AuNPs at pH 2 when compared to pH 7, one of them is the expected difference in reaction rate constant towards Au(III) between e^-_{aq} (dominating at pH 7) and $H^\bullet$ (dominating at pH 2). Such differences have been clearly demonstrated in the case of Ag(I) reduction, where the rate constant of e^-_{aq} is over threefold higher than that of $H^\bullet$ [35]. In the case of chloroaurate, $k = 5.7 \times 10^9$ dm³·mol⁻¹·s⁻¹ has been determined for reduction by $H^\bullet$ [35], while there are data for the solvated electron in 2-propanol indicating that its reaction with chloroaurate is much faster, at $k = 2.6 \times 10^{10}$ dm³·mol⁻¹·s⁻¹ [43]. This difference may be of particular importance when these reactions have to compete with e^-_{aq} and $H^\bullet$ scavenging by oxygen.

Conclusion

Well-defined PHEMA-based networks can be synthesized and used as uniform substrates for *in situ* formation of patterned AuNP-containing nanocomposites. The cross-link density was evidenced as a key factor influencing the dimensions and the overall concentration of AuNPs produced by EB-irradiation at 10 kGy of poly(HEMA) hydrogels swollen with 1 mM aqueous Au(III) solutions.

pH-responsive gels can be obtained by a similar synthetic procedure, using MADQUAT or AA as an ionic co-monomer. Furthermore, temperature-sensitive hydrogels can be obtained in this way by copolymerizing HEMA with NIPAm.

This study stresses the lack of knowledge on the impact of radiation treatment on PHEMA and PHEMA-based networks, in terms of the relative trend for scission and cross-linking, amount of extractables, nature of intermediates, and long-lived reactive species. The precise effects, as well as the nature of long-lived intermediates with potential reductive power towards Au(III) ions, need to be explored in more detail.

The patterned, stimuli-sensitive nanocomposite hydrogels may become a new class of interesting multifunctional materials for electronics, optics, and medicine.

In that perspective, ongoing studies and future developments are currently in progress to gain better control on the conversion of metal salts present in hydrogels into AuNPs of specific size and spatial distribution. Detailed investigation on the nature and amount of remaining active species in the cured xerogels, as well as on the processing conditions by pre-irradiation or simultaneous treatment on the efficiency of reduction reactions should help to go further.

Detailed characterization of the optical properties resulting from the presence of AuNPs in the hydrogels along with their evolution with time, leaching of AuNPs, study of the temperature and
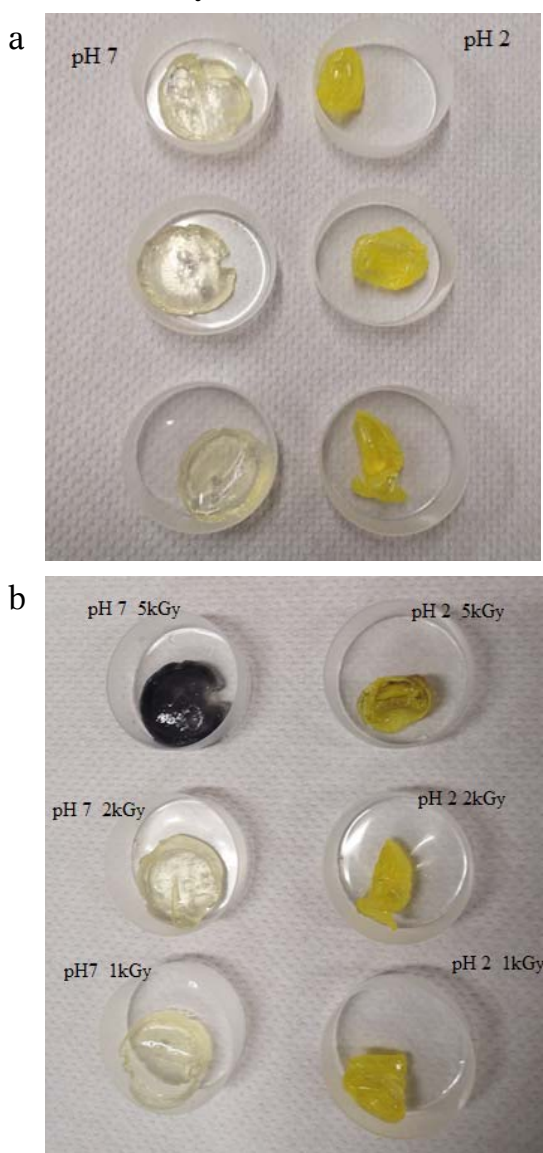

Fig. 14. Poly(HEMA-co-MADQUAT) hydrogels synthesized by UV irradiation (254 nm, irradiance 2.6 mW·cm⁻², exposure dose 8 J·cm⁻²) of a solution composed of 50 vol.% of aqueous 30% hydrogen peroxide, 47.5 vol.% of HEMA/EGDMA (99/1) and 2.5 vol.% of aqueous 75% MADQUAT, (a) non-irradiated and (b) irradiated by EB at various doses after having been soaked in 1 mM Au(III) solutions of pH 2 and pH 7.

pH responsiveness will be helpful for the design of novel patterned nanocomposites with specific functionalities.

ORCID

X. Coqueret http://orcid.org/0000-0002-9645-5506
S. Kadłubowski http://orcid.org/0000-0003-0648-5208
P. Ulański http://orcid.org/0000-0002-4310-3574

References

1. Kelly, K. L., Coronado, E., Zhao, L. L., & Schatz, G. C. (2003). The optical properties of metal nanoparticles: the influence of size, shape, and dielectric environment. *J. Phys. Chem. B*, *107*(3), 668–677.
2. Daniel, M. C., & Astruc, D. (2004). Gold nanoparticles: assembly, supramolecular chemistry, quantum-size-related properties, and applications toward biology, catalysis, and nanotechnology. *Chem. Rev.*, *104*(1), 293–346.
3. García, M. A. (2011). Surface plasmons in metallic nanoparticles: fundamentals and applications. *J. Phys. D-Appl. Phys.*, *44*(28), 283001.
4. Turkevich, J., Stevenson, P. C., & Hillier, J. (1951). A study of the nucleation and growth processes in the synthesis of colloidal gold. *Discus. Faraday Soc.*, *11*, 55–75.
5. Huang, H. H., Yan, F. Q., Kek, Y. M., Chew, C. H., Xu, G. Q., Ji, W., & Tang, S. H. (1997). Synthesis, characterization, and nonlinear optical properties of copper nanoparticles. *Langmuir*, *13*(2), 172–175.
6. Sato-Berrú, R., Redón, R., Vázquez Olmos, A., & Saniger, J. M. (2009). Silver nanoparticles synthesized by direct photoreduction of metal salts. Application in surface-enhanced Raman spectroscopy. *J. Raman Spectrosc.*, *40*(4), 376–380.
7. Sánchez-Iglesias, A., Pastoriza-Santos, I., Pérez-Juste, J., Rodríguez-González, B., Garcia de Abajo, F. J., & Liz-Marzán, L. M. (2006). Synthesis and optical properties of gold nanodecahedra with size control. *Adv. Mater.*, *18*(19), 2529–2534.
8. Belloni, J., Mostafavi, M., Remita, H., Marignier, J. L., & Delcourt, M. O. (1998). Radiation-induced synthesis of mono-and multi-metallic clusters and nanocolloids. *New J. Chem.*, *22*(11), 1239–1255.
9. Abedini, A., Daud, A. R., Hamid, M. A. A., Othman, N. K., & Saion, E. (2013). A review on radiation-induced nucleation and growth of colloidal metallic nanoparticles. *Nanoscale Res. Lett.*, *8*(1), 474.
10. Henglein, A. (1999). Radiolytic preparation of ultra-fine colloidal gold particles in aqueous solution: optical spectrum, controlled growth, and some chemical reactions. *Langmuir*, *15*(20), 6738–6744.
11. Gachard, E., Remita, H., Khatouri, J., Keita, B., Nadjo, L., & Belloni, J. (1998). Radiation-induced and chemical formation of gold clusters. *New J. Chem.*, *22*(11), 1257–1265.
12. Tagawa, S., Hayashi, N., Yoshida, Y., Washio, M., & Tabata, Y. (1989). Pulse radiolysis studies on liquid alkanes and related polymers. *Int. J. Radiat. Appl. Instrum. C-Radiat. Phys. Chem.*, *34*(4), 503–511.
13. Kapoor, S., Lawless, D., Kennepohl, P., Meisel, D., & Serpone, N. (1994). Reduction and aggregation of silver ions in aqueous gelatin solutions. *Langmuir*, *10*(9), 3018–3022.
14. Goldenberg, L. M., Sakhno, O. V., Smirnova, T. N., Helliwell, P., Chechik, V., & Stumpe, J. (2008). Holographic composites with gold nanoparticles: nanoparticles promote polymer segregation. *Chem. Mat.*, *20*(14), 4619–4627.
15. Pardo Yissar, V., Gabai, R., Shipway, A. N., Bourenko, T., & Willner, I. (2001). Gold nanoparticle/hydrogel composites with solvent switchable electronic properties. *Adv. Mater.*, *13*(17), 1320–1323.
16. Wang, C., Flynn, N. T., & Langer, R. (2004). Controlled structure and properties of thermoresponsive nanoparticle–hydrogel composites. *Adv. Mater.*, *16*(13), 1074–1079.
17. Marić, I., Vujičić, N. Š., Pustak, A., Gotić, M., & Jurkin, T. (2020). One-step synthesis of poly (ethylene oxide)/gold nanocomposite hydrogels and suspensions using gamma-irradiation. *Radiat. Phys. Chem.*, *170*, 108657.
18. Bond, G. C., & Thompson, D. T. (2000). Gold-catalysed oxidation of carbon monoxide. *Gold Bull.*, *33*(2), 41–50.
19. Belloni, J. (2006). Nucleation, growth and properties of nanoclusters studied by radiation chemistry: application to catalysis. *Catal. Today*, *113*(3/4), 141–156.
20. Evanoff Jr, D. D., & Chumanov, G. (2005). Synthesis and optical properties of silver nanoparticles and arrays. *ChemPhysChem*, *6*(7), 1221–1231.
21. Vô, K. D. N., Kowandy, C., Dupont, L., & Coqueret, X. (2015). Evidence of chitosan-mediated reduction of Au (III) to Au (0) nanoparticles under electron beam by using OH and e⁻$_{aq}$ scavengers. *Chem. Commun.*, *51*(19), 4017–4020.
22. Li, T., Park, H. G., & Choi, S. H. (2007). γ-Irradiation-induced preparation of Ag and Au nanoparticles and their characterizations. *Mater. Chem. Phys.*, *105*(2/3), 325–330.
23. Zhu, C. -H., Hai, Z. -B., Cui, C. -H., Li, H. -H., Chen, J. -F., & Yu, S. -H. (2012). In situ controlled synthesis of thermosensitive poly(N-isopropylacrylamide)/Au nanocomposite hydrogels by gamma radiation for catalytic application. *Small*, *8*(6), 930–936.
24. Kumaraswamy, S., & Mallaiah, S. H. (2016). Swelling and mechanical properties of radiation crosslinked Au/PVA hydrogel nanocomposites. *Radiat. Eff. Defects Solids*, *171*(11/12), 869–878.
25. Kumaraswamy, S., Srikanth, L. P., & Somashekarappa, H. M. (2020). Swelling and cytocompatibility studies of Au/PVA hydrogel nanocomposites synthesized using gamma irradiation technique. *AIP Conf. Proc.*, *2244*, art. no. 070005.

26. Kumar, M., Varshney, L., & Francis, S. (2005). Radiolytic formation of Ag clusters in aqueous polyvinyl alcohol solution and hydrogel matrix. *Radiat. Phys. Chem.*, *73*(1), 21–27.

27. Henríquez, C. M. G., Guerra, G. D. C. P., Vallejos, M. A. S., de la Fuente, S. D. R., Flores, M. T. U., & Jimenez, L. M. R. (2014). In situ silver nanoparticle formation embedded into a photopolymerized hydrogel with biocide properties. *J. Nanostructure Chem.*, *4*(4), 119–132.

28. Krklješ, A. N., Marinović-Cincović, M. T., Kacarevic-Popovic, Z. M., & Nedeljković, J. M. (2007). Radiolytic synthesis and characterization of Ag-PVA nanocomposites. *Eur. Polym. J.*, *43*(6), 2171–2176.

29. Krklješ, A., Nedeljković, J. M., & Kačarević-Popović, Z. M. (2007). Fabrication of Ag-PVA hydrogel nanocomposite by γ-irradiation. *Polymer Bull.*, *58*(1), 271–279.

30. Jovanović, Ž., Krklješ, A., Stojkovska, J., Tomić, S., Obradović, B., Mišković-Stanković, V., & Kačarević-Popović, Z. (2011). Synthesis and characterization of silver/poly(N-vinyl-2-pyrrolidone) hydrogel nanocomposite obtained by in situ radiolytic method. *Radiat. Phys. Chem.*, *80*(11), 1208–1215.

31. Schulz, G. V., & Harborth, G. (1947). The mechanism of the explosive polymerization of methyl methacrylate. *Die Makromolekulare Chemie*, *1*(1), 106–139.

32. Flory, P. J. (1953). *Principles of polymer chemistry*. Ithaca, NY: Cornell University Press.

33. Campan, R., Cazaux, F., & Coqueret, X. (2002). Controlled swelling of poly(hydroxyethyl methacrylate) hydrogels by photochemical grafting of hydrophobic acrylates. *Macromol. Mater. Eng.*, *287*(12), 924–930.

34. Olejniczak, J., Rosiak, J., & Charlesby, A. (1991). Gel/dose curves for polymers undergoing simultaneous crosslinking and scission. *Radiat. Phys. Chem.*, *37*(3), 499–504.

35. Buxton, G. V., Greenstock, C. L., Helman, W. P., & Ross A. B. (1988). Critical review of rate constants for reactions of hydrated electrons, hydrogen atoms and hydroxyl radicals ($^{\bullet}OH/^{\bullet}O^{-}$) in aqueous solutions. *J. Phys. Chem. Ref. Data*, *17*(2), 513–886.

36. Ilavský, M., Fähnrich, J., Nedbal, J., & Bouchal, K. (1996). Swelling and photoelastic behaviour of ionized hydrogels of poly(acrylic acid). *Polymer Bull.*, *37*, 791–798.

37. Serjeant, E. P., & Dempsey, B. (1979). *Ionisation constants of organic acids in aqueous solution*. New York: Pergamon Press. (IUPAC Chemical Data Series No. 23).

38. Oosawa, F. (1971). *Polyelectrolytes*. New York: Marcel Dekker.

39. Schild, H. G., & Tirrell, D. A. (1990). Microcalorimetric detection of lower critical solution temperatures in aqueous polymer solutions. *J. Phys. Chem.*, *94*, 4352–4356.

40. Alexander, P., Charlesby, A., & Ross, M. (1954). The degradation of solid polymethylmethacrylate by ionizing radiation. *Proc. R. Soc. London Ser. A-Math. Phys. Sci.*, *223*(1154), 392–404.

41. Choi, J. O., Moore, J. A., Corelli, J. C., Silverman, J. P., & Bakhru, H. (1988). Degradation of poly(methyl methacrylate) by deep ultraviolet, X-ray, electron beam, and proton beam irradiations. *J. Vac. Sci. Technol. B*, *6*(6), 2286–2289.

42. Ritger, P. L., & Peppas, N. A. (1987). A simple equation for description of solute release I. Fickian and non-fickian release from non-swellable devices in the form of slabs, spheres, cylinders or discs. *J. Control. Release*, *5*(1), 23–36.

43. Dey, G. R., El Omar, A. K., Jacob, J. A., Mostafavi, M., & Belloni, J. (2011). Mechanism of trivalent gold reduction and reactivity of transient divalent and monovalent gold ions studied by gamma and pulse radiolysis. *J. Phys.Chem. A*, *115*, 383–391.